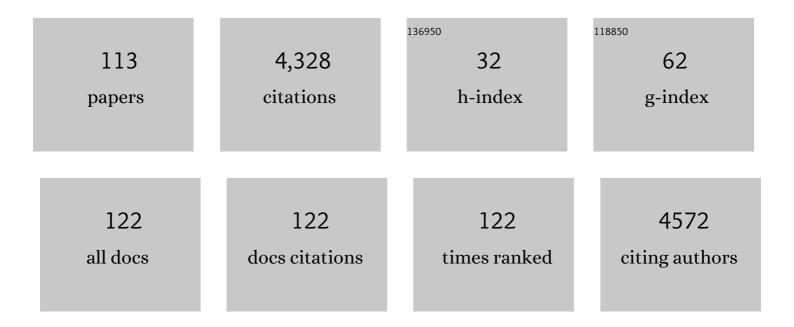
List of Publications by Year in descending order

Source: https://exaly.com/author-pdf/6959695/publications.pdf Version: 2024-02-01



FA-HSUAN LIN

#	Article	IF	CITATIONS
1	Assessing and improving the spatial accuracy in MEG source localization by depth-weighted minimum-norm estimates. NeuroImage, 2006, 31, 160-171.	4.2	420
2	Human posterior auditory cortex gates novel sounds to consciousness. Proceedings of the National Academy of Sciences of the United States of America, 2004, 101, 6809-6814.	7.1	395
3	Task-modulated "what" and "where" pathways in human auditory cortex. Proceedings of the National Academy of Sciences of the United States of America, 2006, 103, 14608-14613.	7.1	315
4	Distributed current estimates using cortical orientation constraints. Human Brain Mapping, 2006, 27, 1-13.	3.6	281
5	Parallel imaging reconstruction using automatic regularization. Magnetic Resonance in Medicine, 2004, 51, 559-567.	3.0	232
6	Spectral spatiotemporal imaging of cortical oscillations and interactions in the human brain. NeuroImage, 2004, 23, 582-595.	4.2	169
7	Lexical influences on speech perception: A Granger causality analysis of MEG and EEG source estimates. Neurolmage, 2008, 43, 614-623.	4.2	153
8	Dynamic retrospective filtering of physiological noise in BOLD fMRI: DRIFTER. NeuroImage, 2012, 60, 1517-1527.	4.2	127
9	PROPELLER EPI: An MRI technique suitable for diffusion tensor imaging at high field strength with reduced geometric distortions. Magnetic Resonance in Medicine, 2005, 54, 1232-1240.	3.0	115
10	Cancellation of EEG and MEG signals generated by extended and distributed sources. Human Brain Mapping, 2010, 31, 140-149.	3.6	111
11	Onset timing of crossâ€sensory activations and multisensory interactions in auditory and visual sensory cortices. European Journal of Neuroscience, 2010, 31, 1772-1782.	2.6	107
12	Attention-driven auditory cortex short-term plasticity helps segregate relevant sounds from noise. Proceedings of the National Academy of Sciences of the United States of America, 2011, 108, 4182-4187.	7.1	99
13	Dynamic magnetic resonance inverse imaging of human brain function. Magnetic Resonance in Medicine, 2006, 56, 787-802.	3.0	93
14	Enhanced Spontaneous Oscillations in the Supplementary Motor Area Are Associated with Sleep-Dependent Offline Learning of Finger-Tapping Motor-Sequence Task. Journal of Neuroscience, 2013, 33, 13894-13902.	3.6	80
15	Sensitivity-encoded (SENSE) proton echo-planar spectroscopic imaging (PEPSI) in the human brain. Magnetic Resonance in Medicine, 2007, 57, 249-257.	3.0	78
16	Primary and multisensory cortical activity is correlated with audiovisual percepts. Human Brain Mapping, 2010, 31, 526-538.	3.6	72
17	A wavelet-based approximation of surface coil sensitivity profiles for correction of image intensity inhomogeneity and parallel imaging reconstruction. Human Brain Mapping, 2003, 19, 96-111.	3.6	68
18	Accelerated proton echo planar spectroscopic imaging (PEPSI) using CRAPPA with a 32â€channel phasedâ€array coil. Magnetic Resonance in Medicine, 2008, 59, 989-998.	3.0	63

#	Article	IF	CITATIONS
19	Multivariate analysis of neuronal interactions in the generalized partial least squares framework: simulations and empirical studies. NeuroImage, 2003, 20, 625-642.	4.2	54
20	Functional MRI using regularized parallel imaging acquisition. Magnetic Resonance in Medicine, 2005, 54, 343-353.	3.0	48
21	Event-related single-shot volumetric functional magnetic resonance inverse imaging of visual processing. Neurolmage, 2008, 42, 230-247.	4.2	45
22	Brain hemodynamic activity during viewing and re-viewing of comedy movies explained by experienced humor. Scientific Reports, 2016, 6, 27741.	3.3	43
23	Dynamic Granger–Geweke causality modeling with application to interictal spike propagation. Human Brain Mapping, 2009, 30, 1877-1886.	3.6	42
24	MRI-constrained spectral imaging of benzodiazepine modulation of spontaneous neuromagnetic activity in human cortex. NeuroImage, 2007, 35, 577-582.	4.2	41
25	Stimulus-induced Rotary Saturation (SIRS): A potential method for the detection of neuronal currents with MRI. NeuroImage, 2008, 42, 1357-1365.	4.2	41
26	PROPELLER-EPI with parallel imaging using a circularly symmetric phased-array RF coil at 3.0 T: Application to high-resolution diffusion tensor imaging. Magnetic Resonance in Medicine, 2006, 56, 1352-1358.	3.0	40
27	Accelerated shortâ€TE 3D proton echoâ€planar spectroscopic imaging using 2Dâ€SENSE with a 32â€channel array coil. Magnetic Resonance in Medicine, 2007, 58, 1107-1116.	3.0	40
28	Parallel input makes the brain run faster. NeuroImage, 2008, 40, 1792-1797.	4.2	40
29	Ultrafast inverse imaging techniques for fMRI. NeuroImage, 2012, 62, 699-705.	4.2	40
30	Spatially sparse source cluster modeling by compressive neuromagnetic tomography. NeuroImage, 2010, 53, 146-160.	4.2	38
31	fMRI hemodynamics accurately reflects neuronal timing in the human brain measured by MEG. NeuroImage, 2013, 78, 372-384.	4.2	36
32	Linear constraint minimum variance beamformer functional magnetic resonance inverse imaging. Neurolmage, 2008, 43, 297-311.	4.2	35
33	Whole-head rapid fMRI acquisition using echo-shifted magnetic resonance inverse imaging. NeuroImage, 2013, 78, 325-338.	4.2	35
34	Singleâ€shot magnetic resonance spectroscopic imaging with partial parallel imaging. Magnetic Resonance in Medicine, 2009, 61, 541-547.	3.0	34
35	Enhanced neural synchrony between left auditory and premotor cortex is associated with successful phonetic categorization. Frontiers in Psychology, 2014, 5, 394.	2.1	34
36	Relative latency and temporal variability of hemodynamic responses at the human primary visual cortex. NeuroImage, 2018, 164, 194-201.	4.2	34

#	Article	IF	CITATIONS
37	Fast mapping of theT2 relaxation time of cerebral metabolites using proton echo-planar spectroscopic imaging (PEPSI). Magnetic Resonance in Medicine, 2007, 57, 859-865.	3.0	33
38	Reconstruction of MRI data encoded by multiple nonbijective curvilinear magnetic fields. Magnetic Resonance in Medicine, 2012, 68, 1145-1156.	3.0	31
39	Significant feed-forward connectivity revealed by high frequency components of BOLD fMRI signals. NeuroImage, 2015, 121, 69-77.	4.2	31
40	Cognitive impairment and hippocampal atrophy in chronic kidney disease. Acta Neurologica Scandinavica, 2017, 136, 477-485.	2.1	30
41	Parallel MRI reconstruction using variance partitioning regularization. Magnetic Resonance in Medicine, 2007, 58, 735-744.	3.0	28
42	Increasing fMRI Sampling Rate Improves Granger Causality Estimates. PLoS ONE, 2014, 9, e100319.	2.5	28
43	Magnetoencephalographic Mapping of Interictal Spike Propagation: A Technical and Clinical Report. American Journal of Neuroradiology, 2007, 28, 1486-1488.	2.4	26
44	Physiological noise reduction using volumetric functional magnetic resonance inverse imaging. Human Brain Mapping, 2012, 33, 2815-2830.	3.6	26
45	K-space reconstruction of magnetic resonance inverse imaging (K-InI) of human visuomotor systems. NeuroImage, 2010, 49, 3086-3098.	4.2	23
46	Premature white matter aging in patients with right mesial temporal lobe epilepsy: A machine learning approach based on diffusion MRI data. NeuroImage: Clinical, 2019, 24, 102033.	2.7	22
47	Superresolution parallel magnetic resonance imaging: Application to functional and spectroscopic imaging. NeuroImage, 2009, 47, 220-230.	4.2	21
48	Effective Cerebral Connectivity during Silent Speech Reading Revealed by Functional Magnetic Resonance Imaging. PLoS ONE, 2013, 8, e80265.	2.5	20
49	Multidimensionally encoded magnetic resonance imaging. Magnetic Resonance in Medicine, 2013, 70, 86-96.	3.0	19
50	Degenerate mode birdcage volume coil for sensitivity-encoded imaging. Magnetic Resonance in Medicine, 2003, 50, 1107-1111.	3.0	18
51	Simultaneous multi-slice inverse imaging of the human brain. Scientific Reports, 2017, 7, 17019.	3.3	17
52	Reduced synchronized brain activity in schizophrenia during viewing of comedy movies. Scientific Reports, 2019, 9, 12738.	3.3	15
53	Anatomically and Functionally Constrained Minimum-Norm Estimates. , 2010, , 186-215.		14
54	Quantitative spectral/spatial analysis of phased array coil in magnetic resonance imaging based on method of moment. IEEE Transactions on Medical Imaging, 1999, 18, 1129-1137.	8.9	13

#	Article	IF	CITATIONS
55	Quantitative analysis of magnetic resonance radio-frequency coils based on method of moments. IEEE Transactions on Magnetics, 1999, 35, 2118-2127.	2.1	12
56	Sparse current source estimation for MEG using loose orientation constraints. Human Brain Mapping, 2013, 34, 2190-2201.	3.6	12
57	Dissociable Influences of Auditory Object vs. Spatial Attention on Visual System Oscillatory Activity. PLoS ONE, 2012, 7, e38511.	2.5	12
58	Functional and effective connectivity of visuomotor control systems demonstrated using generalized partial least squares and structural equation modeling. Human Brain Mapping, 2009, 30, 2232-2251.	3.6	11
59	An orthogonal shim coil for 3T brain imaging. Magnetic Resonance in Medicine, 2020, 83, 1499-1511.	3.0	11
60	Feature-dependent intrinsic functional connectivity across cortical depths in the human auditory cortex. Scientific Reports, 2018, 8, 13287.	3.3	9
61	Impact of physiological noise in characterizing the functional MRI default-mode network in Alzheimer's disease. Journal of Cerebral Blood Flow and Metabolism, 2021, 41, 166-181.	4.3	9
62	Distributed source modeling of intracranial stereoelectro-encephalographic measurements. Neurolmage, 2021, 230, 117746.	4.2	9
63	Hippocampal Atrophy Is Associated with Altered Hippocampus–Posterior Cingulate Cortex Connectivity in Mesial Temporal Lobe Epilepsy with Hippocampal Sclerosis. American Journal of Neuroradiology, 2017, 38, 626-632.	2.4	8
64	Functional magnetic resonance inverse imaging of human visuomotor systems using eigenspace linearly constrained minimum amplitude (eLCMA) beamformer. NeuroImage, 2011, 55, 87-100.	4.2	7
65	Multi-projection magnetic resonance inverse imaging of the human visuomotor system. NeuroImage, 2012, 61, 304-313.	4.2	7
66	Noise amplification in parallel wholeâ€head ultraâ€lowâ€field magnetic resonance imaging using 306 detectors. Magnetic Resonance in Medicine, 2013, 70, 595-600.	3.0	7
67	Decoupled dynamic magnetic field measurements improves diffusion-weighted magnetic resonance images. Scientific Reports, 2017, 7, 11630.	3.3	7
68	Suppressing Multi-Channel Ultra-Low-Field MRI Measurement Noise Using Data Consistency and Image Sparsity. PLoS ONE, 2013, 8, e61652.	2.5	6
69	Efficient concomitant and remanence field artifact reduction in ultraâ€lowâ€field MRI using a frequencyâ€space formulation. Magnetic Resonance in Medicine, 2014, 71, 955-965.	3.0	6
70	Reduction of lipid contamination in MR spectroscopy imaging using signal space projection. Magnetic Resonance in Medicine, 2019, 81, 1486-1498.	3.0	6
71	A Flexible and Modular Receiver Coil Array for Magnetic Resonance Imaging. IEEE Transactions on Medical Imaging, 2019, 38, 824-833.	8.9	6
72	Trail Making Test Performance Using a Touch-Sensitive Tablet: Behavioral Kinematics and Electroencephalography. Frontiers in Human Neuroscience, 2021, 15, 663463.	2.0	6

FA-HSUAN LIN

#	Article	IF	CITATIONS
73	Improving the spatial resolution of magnetic resonance inverse imaging via the blipped-CAIPI acquisition scheme. NeuroImage, 2014, 91, 401-411.	4.2	5
74	Mitigate <i>B</i> ₁ ⁺ inhomogeneity using spatially selective radiofrequency excitation with generalized spatial encoding magnetic fields. Magnetic Resonance in Medicine, 2014, 71, 1458-1469.	3.0	5
75	The sequence of cortical activity inferred by response latency variability in the human ventral pathway of face processing. Scientific Reports, 2018, 8, 5836.	3.3	5
76	Seizure Frequency Is Associated with Effective Connectivity of the Hippocampal–Diencephalic–Cingulate in Epilepsy with Unilateral Mesial Temporal Sclerosis. Brain Connectivity, 2021, 11, 457-470.	1.7	5
77	Processing of an Audiobook in the Human Brain Is Shaped by Cultural Family Background. Brain Sciences, 2022, 12, 649.	2.3	4
78	Long-Range Coupling of Prefrontal Cortex and Visual (MT) or Polysensory (STP) Cortical Areas in Motion Perception. IFMBE Proceedings, 2010, , 298-301.	0.3	3
79	Mitigate B <inf>1</inf> ⁺ inhomogeneity by nonlinear gradients and RF shimming. , 2013, 2013, 1085-8.		3
80	A 32-Channel Head Coil Array with Circularly Symmetric Geometry for Accelerated Human Brain Imaging. PLoS ONE, 2016, 11, e0149446.	2.5	3
81	The neural mechanism underpinning balance calibration between action inhibition and activation initiated by reward motivation. Scientific Reports, 2017, 7, 9722.	3.3	3
82	Removing signal intensity inhomogeneity from surface coil MRI using discrete wavelet transform and wavelet packet. , 0, , .		2
83	Magnetic resonance imaging receiver coil decoupling using circumferential shielding structures. , 2016, 2016, 6254-6257.		2
84	Incongruent pitch cues are associated with increased activation and functional connectivity in the frontal areas. Scientific Reports, 2018, 8, 5206.	3.3	2
85	Differential brain mechanisms during reading human vs. machine translated fiction and news texts. Scientific Reports, 2019, 9, 13251.	3.3	2
86	Concurrent electrophysiological and hemodynamic measurements of evoked neural oscillations in human visual cortex using sparsely interleaved fast fMRI and EEG. NeuroImage, 2020, 217, 116910.	4.2	2
87	Multivariate Identification of Functional Neural Networks Underpinning Humorous Movie Viewing. Frontiers in Psychology, 2020, 11, 547353.	2.1	2
88	Ultra-Low-Field MRI and Its Combination with MEG. , 2014, , 941-972.		2
89	Modeling Adaptation Effects in fMRI Analysis. Lecture Notes in Computer Science, 2009, 12, 1009-1017.	1.3	2

#	Article	IF	CITATIONS
91	Imaging of oscillatory cortical activity using combined MEG and fMRI. International Congress Series, 2007, 1300, 19-22.	0.2	1
92	Rotary scanning acquisition in ultraâ€lowâ€field MRI. Magnetic Resonance in Medicine, 2016, 75, 2255-2264.	3.0	1
93	Integrated RF-shim coil allowing two degrees of freedom shim current. , 2016, 2016, 6246-6249.		1
94	Mitigation of B1+ inhomogeneity using spatially selective excitation with jointly designed quadratic spatial encoding magnetic fields and RF shimming. Magnetic Resonance in Medicine, 2017, 78, 577-587.	3.0	1
95	Combining Noninvasive Electromagnetic and Hemodynamic Measures of Human Brain Activity. , 2021, , 179-193.		1
96	The impulse noise of TMS inside a 3 T and 9.4 T MRI. Brain Stimulation, 2021, 14, 1606.	1.6	1
97	Ballistocardiogram suppression in concurrent <scp>EEGâ€MRI</scp> by dynamic modeling of heartbeats. Human Brain Mapping, 0, , .	3.6	1
98	Quantitative spatial/spectral analysis of magnetic resonance imaging surface and phased array coils of arbitrary geometry based on method of moment. , 0, , .		0
99	Correction to "Quantitative analysis of magnetic resonance radio-frequency coils based on method of moment". IEEE Transactions on Magnetics, 2000, 36, 410-410.	2.1	0
100	Dynamic Frequency-Domain Conditional Granger Causality Applied to Magnetoencephalography. NeuroImage, 2009, 47, S148.	4.2	0
101	MEG cortical activation during sleep correlated with improvement of a motor sequence learning. Neuroscience Research, 2010, 68, e77.	1.9	0
102	Ultra-low-field magnetic resonance imaging combined with magnetoencephalography. , 2011, , .		0
103	Combination of MEG and MRI in one setup. Biomedizinische Technik, 2012, 57, .	0.8	Ο
104	Combining parallel detection of proton echo planar spectroscopic imaging (PEPSI) measurements with a data-consistency constraint improves SNR. NMR in Biomedicine, 2015, 28, 1678-1687.	2.8	0
105	The Compressible Estimate (CE) of MEG Current Sources. Frontiers in Neuroscience, 0, 4, .	2.8	0
106	The Compressible Estimate (CE) of MEG Current Sources. IFMBE Proceedings, 2010, , 159-162.	0.3	0
107	Assessing causal interaction in human brain using conditional mutual information and transfer entropy. Frontiers in Neuroscience, 0, 4, .	2.8	0
108	Parallel Magnetic Resonance Imaging Acquisition and Reconstruction: Application to Functional and Spectroscopic Imaging in Human Brain. , 2011, , 245-262.		0

#	Article	IF	CITATIONS
109	Deficient Emotional Intelligence and Dysfunctional Early Emotional Prosody Processing Varying with the Severity of Auditory Hallucinations in Schizophrenics. Neuropsychiatry, 2018, 08, .	0.4	0
110	Ultra-Low-Field MRI and Its Combination with MEC. , 2019, , 1-33.		0
111	Ultra-Low-Field MRI and Its Combination with MEG. , 2019, , 1261-1293.		0
112	Hemodynamic changes in response to excitatory and inhibitory modulations by transcranial magnetic stimulation at the human sensorimotor cortex. Brain Stimulation, 2021, 14, 1611-1612.	1.6	0
113	Investigating the genesis of evoked responses by invasive electrophysiological recording and direct stimulation in the human brain. Brain Stimulation, 2021, 14, 1685.	1.6	0